



# Effect of Inhibitor UNC0642 on Expression of G9a and Its Proliferative and Apoptotic Markers in Breast Cancer Cell Line MCF-7

Affifa Yaqub<sup>1</sup>, Mehroze Amin<sup>1</sup>, Qindeel Fatima<sup>1</sup>, Rabail Hassan Toor<sup>1,3</sup>, Saira Aftab<sup>1</sup> and Abdul Rauf Shakoori<sup>1,2\*</sup>

<sup>1</sup>School of Biological Sciences, University of the Punjab, Quaid-i-Azam Campus, Lahore 54590, Pakistan

<sup>2</sup>Cancer Research Centre, University of the Punjab, Quaid-i-Azam Campus, Lahore 54590, Pakistan

<sup>3</sup>UVM Cancer Center, Larner College of Medicine, Department of Biochemistry, University of Vermont, Burlington, VT 05405, USA

## ABSTRACT

G9a is a lysine methyltransferase that has been reported to downregulate the expression of tumor suppressor genes in a variety of cancerous cells. The present study explores the anti-cancer activity of UNC0642, a novel potent inhibitor of G9a in MCF-7 breast cancer cell line. Analysis of growth and proliferation parameters by various cell-based assays such as neutral red assay and BrdU cell proliferation assay showed that higher concentrations were lethal for the cancerous cells. IC<sub>50</sub> was found to be 12.6 μM. Further contextualization of the therapeutic potential of G9a inhibition was provided by expression analysis of the G9a gene and genes associated with cell proliferation, tumor suppression, and apoptosis. The gene expression of fibroblast growth factor 1 (FGF1), enolase 2 (ENO2), cyclin D1 (CCND1), catalytic subunit of AMP-activated protein kinase (AMPKα2), RNA polymerase II transcription elongation factor (ELL2), and pro-apoptotic Bcl-2 homology 3-only protein (BIM) in MCF-7 breast cancer and normal human embryonic kidney HEK-293 cell lines were studied in response to treatment with different concentrations of UNC0642. Inhibition of G9a expression was observed in a dose-dependent manner in both cell lines with increasing UNC0642 concentrations. A dose-dependent downregulation of gene expression of proliferation marker genes (FGF-1, CCND1, and ENO2) was observed in both cell lines, whereas upregulation of tumor suppressor genes (AMPKα2 and ELL2) and apoptotic marker gene (BIM) was observed in a dose-dependent manner. Taken together, the results indicated the potential of G9a inhibition in the reduction of cancerous cell proliferation and inducing apoptosis in cancerous cells. Further elucidation of the signaling pathways associated with G9a, in-vitro and in-vivo safety analyses is required to fully establish G9a as a therapeutic target for cancer progression and UNC0642 as an anti-cancerous therapeutic agent for the treatment of breast cancer.

## Article Information

Received 12 May 2022

Revised 28 May 2022

Accepted 14 June 2022

Available online 11 August 2022

(early access)

Published 23 August 2022

## Authors' Contribution

Conceptualization, fund acquisition, project administration, resources, supervision: ARS; Investigation, writing original draft: AY; Methodology: MA, QF; Writing (review and editing): ARS, RHT, SA.

All authors read and approved the final manuscript.

## Key words

Breast cancer, Methyltransferase, Fibroblast growth factor, Enolase2, CyclinD1, Bcl2, G9a, UNC0642, AMPKα2, Transcription factors

## INTRODUCTION

G9a is a lysine methyltransferase whose primary function is to di-methylate lysine 9 of histone H3 lysine 9 mono- and di-methyltransferase. G9a-mediated lysine methylation is linked to transcriptional repression

(Casciello *et al.*, 2015). It has been reported that overexpression of G9a is linked to a variety of unusual biological processes as well as to the onset of diseases, including cancer such as breast, ovarian, lung, gastric, hepatocellular, colorectal, and bladder. It takes part in numerous cellular processes and causes cell proliferation, cell invasion, and survival. G9a upregulation increases methylation, which causes major tumor suppressor genes to be downregulated in different cancers, resulting in the inhibition of significant tumor suppressor genes (Rahman *et al.*, 2021). G9a appears to play a significant role in the formation of tumors. Repressing cancer cell proliferation by focusing on G9a and its epigenetic machinery could work with the re-expression of cancer silencer genes. Because of its significant role, it has been considered as a novel target for anti-cancer agents. For this purpose, various G9a inhibitors have been reported that have

\* Corresponding author: arshakoori.sbs@pu.edu.pk, arshaksbs@yahoo.com  
0030-9923/2022/0006-2745 \$ 9.00/0



Copyright 2022 by the authors. Licensee Zoological Society of Pakistan.

This article is an open access article distributed under the terms and conditions of the Creative Commons Attribution (CC BY) license (<https://creativecommons.org/licenses/by/4.0/>).

different pharmacokinetic properties. Some are discovered from natural compounds and others are synthetically made with the ability to block the catalytic activity of G9a (Kaniskan *et al.*, 2018).

BIX01294 was the first studied selective G9a/GLP inhibitor found by high-throughput screening. With an  $IC_{50}$  of 1.7 mM for G9a and 38 mM for GLP, BIX01294 inhibited G9a and GLP selectively (Kubicek *et al.*, 2007). Pharmacologically BIX-01294 inhibits the activity of the G9a gene by triggering cell cycle arrest, activating cellular apoptosis, and inhibiting cellular proliferation during cancer development. Importantly, it was found that the treatment of BIX-01294 differentiates the goat adipose mesenchymal stem cells into nerve cells and adipocytes (Wang *et al.*, 2018). BIX-01294 functions as an epigenetic modifier that can treat myeloid leukemia. BIX-01294 pharmacologically inhibits G9a histone methyltransferase activity to treat certain vascular disorders by changing the structure of microvascular endothelial cells. Recent studies have shown that BIX-01294 can repress tumor growth in NPCs (nasopharyngeal carcinoma cells) and OSCC (oral squamous cells carcinoma) by regulating caspase-independent apoptotic pathways and suppressing autophagic flux. G9a inhibition by BIX-01294 helps in reducing corneal angiogenesis by blocking the production of Nox-4 (NADPH oxidase 4) dependent reactive oxygen species (Li *et al.*, 2021). Treatment with BIX-01294 was demonstrated to inhibit tumor growth in leukemia cell lines HL-60 and NB4 (Savickiene *et al.*, 2014). Zhong *et al.* (2015) reported that anti-apoptotic proteins like Bcl-2 and Mcl1 were reduced in expression while pro-apoptotic proteins like BAX and BAD were increased in expression when G9a was depleted or its activity was suppressed by BIX-01294. BIX-01294 also stimulates autophagy in breast cancer, squamous cell carcinoma of the head and neck, and neuroblastoma cells. However, BIX01294 is selective for GLP over G9a and had inherent toxic effects that were unrelated to the suppression of G9a-mediated methylation. As a result, by using the crystal structure of the protein complex, more efficient G9a inhibitors have been developed, including UNC0224, UNC0321, and E72. Furthermore, UNC0638 and UNC0642 were developed from this class of compounds in order to generate stronger and more selective G9a inhibitors. UNC0642 inhibited G9a with  $IC_{50}$  of <2.5nM and have better selectivity and in vivo pharmacokinetics characteristics than other G9a-specific inhibitors, which makes it a good candidate for the studies of animals (Cao *et al.*, 2019).

The current study investigated the effect of novel inhibitor UNC0642 on the expression of G9a gene and genes associated with proliferation i.e., fibroblast growth factor 1 (FGF1), enolase 2 (ENO2) cyclin D1 (CCND1),

and apoptotic and tumor suppressor genes i.e., catalytic subunit of AMP-activated protein kinase (Ampk $\alpha$ 2), a proapoptotic Bcl-2 homology 3-only protein BIM and RNA polymerase II transcription elongation factor ELL2 in MCF-7 breast cancer and HEK-293 normal human cell lines. In this study, G9a was found to be overexpressed in breast cancer cell line MCF-7 by regulating cell proliferation and apoptosis. UNC0642 reduced breast cancer cell proliferation while promoting apoptosis in vitro by targeting G9a activity. These findings offer insights into G9a inhibition as a probable target for the remedy of most cancers, in particular, breast cancers.

## MATERIALS AND METHODS

### *Cell lines and reagents*

Human Breast Cancer cell line MCF-7 (Cat. No.HTB-22™) and normal Human Embryonic Kidney cell line HEK-293 (Cat. No. CRL-1573™) were purchased from the American Type Culture Collection Manassas, VA, USA. All cell lines were cryopreserved in liquid nitrogen and cultured in complete medium i.e., DMEM (Dulbecco's Modified Eagle Medium–Gibco Cat. No.11965092, Thermo fisher Scientific, Waltham, MA, USA) containing 10% Fetal Bovine Serum (Gibco, Cat. No.12483020) and 1% Penicillin/Streptomycin solution (Gibco, Cat.No.15140122). The cultured cell lines were maintained in a humidified incubator at 37°C having 5% CO<sub>2</sub>. The chemical compound inhibitor UNC0642 with >98% purity was ordered from AdooQ® Biosciences, USA (Cat. No. A15487).

### *Neutral red assay for cell viability*

Neutral red assay was used to determine cell viability. The dye used in the experiment was a neutral red dye (Cat. No. N4638 from Sigma-Aldrich Corporation of America 15 Fleetwood Court Ronkonkoma, NY 11779). At a density of 3,000 cells/cm<sup>2</sup>, MCF-7 cells were seeded in triplicate on 24-well plates (Nunc). The cells were given treatment of different selected concentrations of inhibitor UNC0642 (1μM, 5μM, 10μM, 15μM, and 20μM) after 24 h, and incubated for 48 h along with appropriate controls i.e., cells treated with 0.05% DMSO and cells grown in complete growth medium (untreated). Neutral red assay was performed by following the protocol mentioned in a paper (Ates *et al.*, 2017). The absorbance at 540 nm was measured with a BioTek® ELx808 absorbance microplate reader and mean absorbance value was computed. Background absorbance was subtracted and percentage cell viability was standardized to the DMSO control. GraphPad Prism software (v 7.03) was used to plot the percentage cell viability against UNC0642 inhibitor

concentrations. Furthermore, Microsoft Excel was used to calculate the percentage growth inhibition. The  $IC_{50}$  of UNC0642 was determined by plotting a dose-dependent logarithmic graph of UNC0642 concentrations versus % cell viability.

#### BrdU assay for cell proliferation

The Abcam Cell Proliferation Assay kit (Cat. No. ab126556, 1 Kendall Square, Suite B2304, Cambridge, MA 02139-1517 the USA) was used to perform the cell proliferation assay. BrdU (Bromodeoxyuridine/ 5-Bromo-2'-deoxyuridine) is inserted into replicating DNA during the BrdU assay and can be identified with anti-BrdU antibodies. At a density of 3,000 cells/cm<sup>2</sup>, MCF-7 cells were seeded in triplicate on 24-well plates (Nunc). After 24 h, the cells were treated for 48 h with DMSO (Control) or UNC0642 at the stated concentrations. BrdU assay was carried out following the instructions provided by the Abcam protocol for the use of products. The absorbance at 450 nm was measured with a BioTek® ELx808 absorbance microplate reader and the mean value was computed. The percentage cell proliferation was standardized to the DMSO control after subtracting background absorbance and GraphPad Prism software (v 7.03) was used to plot the % cell proliferation against UNC0642 inhibitor concentrations.

#### Treatment of cells with G9a inhibitor UNC0642

MCF-7 and HEK-293 cells had been seeded at a density of 5000 cells/cm<sup>2</sup> in 6-well plates and incubated for 24 h under normal conditions. The medium was removed after 24 h and wells were washed with 1ml of 1x PBS. Cells in each well were treated with different selected concentrations of inhibitor along with appropriate controls. The 0.05% dimethyl sulphoxide (DMSO) treated cells were used as experimental control and untreated cells were labelled as negative control in this experiment. Each concentration was given in triplicates to treat MCF-7 and HEK-293 cells. After treatment of cells for 48 h, the medium was removed, and cells were collected for each concentration by adding 1ml of ice-chilled TRIzol-reagent in each well.

#### Gene expression analysis using quantitative real-time PCR

The conventional TRIzol™ method for RNA isolation (Simms *et al.*, 1993) was used to extract total RNA from treated cell pellets and Thermo Scientific RevertAid First Strand cDNA Synthesis kit (Cat. No. K1622) was used to make cDNA from 1 µg of RNA in 20 µl reaction. To measure relative gene expression, real-time PCR was successfully done in the Thermo Scientific-96 well PikoReal time machine for triplicates of each cDNA sample using the

SYBR green technique. HMBS was used as a reference gene. The primers shown in Table I were designed by using an online primer designing tool, Primer Blast from NCBI <https://www.ncbi.nlm.nih.gov/tools/primer-blast/>.

**Table I. List of primers used in this study.**

Target genes	Primer Sequences 5'-3'	T <sub>m</sub> (°C)	GC (%)	Product size (bp)
<i>G9a</i>	CCA ACTCTCTACTGGGCTGA	60.5	55	106
	TCCTCTGGTTTCCTTCTCCA	58.4	50	
<i>Ampk</i> <i>α 2</i>	GGCGAACCATCTCAATGTAA	56.4	45	117
	GGGGCATAAACACAGCATAA	56.4	45	
<i>BIM</i>	GCTCTTTCTCTGTGCCTGCT	60.5	55	133
	CCCTCCTCACTTTCCTGCT	60.5	55	
<i>ELL2</i>	CAACCTATCTGCCATCTCA	58.4	50	147
	ATTTGTCTTGCTGGTCTCA	56.4	45	
<i>CCND</i> <i>1</i>	GAGGTGGCAAGAGTGTGGAG	62.5	62.5	150
	CCTGGAAGTCAACGGTAGCA	60.5	60.5	
<i>FGF1</i>	GCAAAAAGTGGGGCTAAATGA	56.4	45	107
	TTGGGGGAATCAGATAGG	58.4	50	
<i>ENO2</i>	TTCCGCACTTTCCTTCTT	56.4	45	142
	AACACCTCAGCACACCAACC	60.5	55	
<i>HMBS</i>	TACCCCGAGAGGAGAGAACA	59.8	55	203
	CGAGCAGGAAGACCAGAAAC	60.0	55	

#### Data analysis

Data were represented as mean ± SD of all triplicates for each experiment. For the cell viability and proliferation assays statistical analysis, when required, were carried out by one-way Analysis of Variance (ANOVA), followed by Dunnett's test with 95% confidence interval and statistical significance of  $p \leq 0.05$  using GraphPad Prism software (v 7.03). For real-time data analysis, data were represented as mean ± SD of all technical and biological replicates and  $\Delta\Delta CT$  method ( $2^{-\Delta\Delta CT}$ ) was used to calculate relative gene expression. Statistical analysis, when required, were carried out by two-way Analysis of Variance (ANOVA), followed by multiple comparisons by Tukey's test using GraphPad Prism software (v 7.03). P-values were presented on graphs as: \*( $p < 0.05$ ), \*\*( $p < 0.01$ ), \*\*\*( $p < 0.005$ ), \*\*\*\*( $p < 0.001$ ).

## RESULTS

#### Morphology of cell lines

Figure 1 shows the characteristic epithelial cell like morphology of breast cancer cell line MCF-7 and normal human embryonic kidney cell line HEK-293 cells.

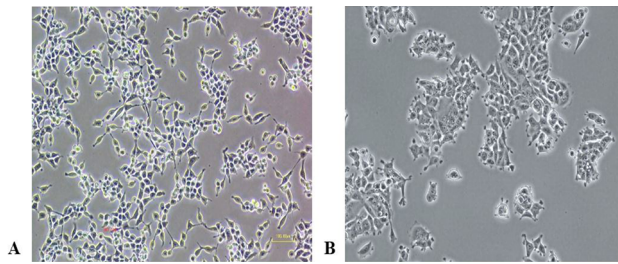


Fig. 1. Morphology of HEK-293 (A) and MCF-7 cell lines (B). Both of these cell lines show normal epithelial cells like morphology. Magnification: 10X.

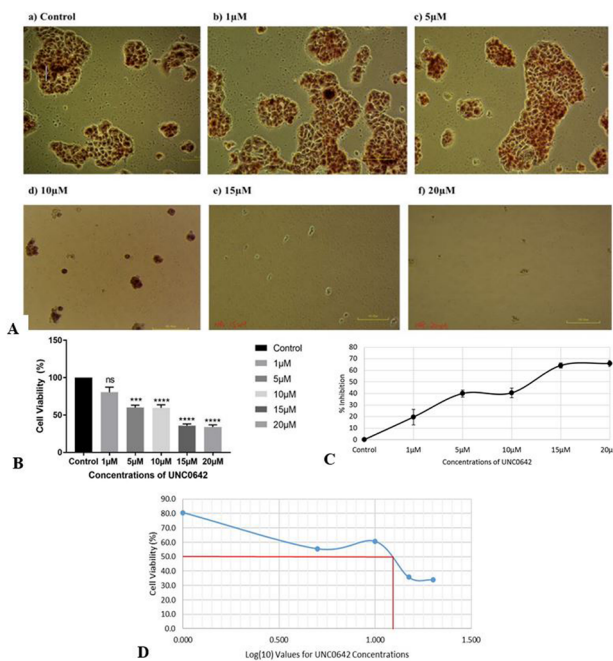


Fig. 2. Effect of different concentrations of UNC0642 on the cell viability of MCF-7 cells (A) determined by Neutral Red assay. The control cells were given medium supplemented with 0.05 percent DMSO. (B) shows percentage cell viability. Taking control as 100 percent, the percentage cell viability was computed. GraphPad Prism (version 7) was used for statistical analysis, with one-way ANOVA and Dunnett's test for multiple comparisons. The data were presented as a mean standard deviation of replicates. ( $P \geq 0.05$ ; ns = not significant,  $*P \leq 0.05$ ,  $**P \leq 0.01$ ,  $***P \leq 0.001$ ,  $****P \leq 0.0001$ ). (C) shows the percentage growth inhibition of MCF-7 cells treated with different concentrations of UNC0642. (D) shows logarithmic curve for determination of  $IC_{50}$  of UNC0642 by neutral red assay against the logarithmic values of the concentrations of UNC0642 selected for the present study. Determination of  $LC_{50}$  was done by calculating anti-log value for the value on x-axis (anti-log 1.1) against 50% cell viability (as indicated by red lines).

#### Effect of UNC0642 inhibitor on cell viability

MCF-7 cells showed normal morphology after treatment with 1 µM concentration of UNC0642 inhibitor. However, the cells treated with 5 µM and 10 µM inhibitor exhibited stressed morphology and reduced viability, whereas very few cells survived after treatment with 15 and 20 µM inhibitor (Fig. 2). Figure 2A shows dose-dependent decreasing cell viability with the increasing concentration of UNC0642. Compared to the control, the MCF-7 cells treated with 1 µM UNC0642 showed 81% viability (Fig. 2B). However, with the increase in the concentration of inhibitor, a significant ( $p \leq 0.05$ ) reduction in cell viability was observed. The viability of cells was significantly ( $P \leq 0.05$ ) reduced to 40% in the presence of 5 µM and 10 µM concentration of the inhibitor, and to 64 and 66% respectively in the presence of 15 µM and 20 µM concentration of inhibitor (Fig. 2B). Figure 2C shows increasing growth inhibition with increasing concentrations of the inhibitor, while Figure 2D shows inhibitory concentrations at which 50% cells were viable ( $IC_{50}$ ) of UNC0642 which was calculated to be 12.6 µM for MCF-7 cells.

#### Effect of UNC0642 on proliferation of MCF-7 breast cancer cells

Figure 3 shows the effect of UNC0642 on proliferation of MCF-7 as well as HEK-293 cells. Both cell lines cells exhibited a significant decrease in the number of cells as the concentration of inhibitor increased. At concentrations 10 µM, 15 µM, and 20 µM the most visible reduction in the number of cells was observed. Moreover, compared to the controls, the cells appeared to be stressed, smaller in size with elongated morphology (Fig. 3A). Treatment with 1 µM inhibitor did not cause any significant ( $P \geq 0.05$ ) decrease in cell proliferation, while treatment of cells with 5 µM and 10 µM decreased cell proliferation by 17% and 22%, respectively. A drastic reduction in cell proliferation was observed at 15 µM (-54.4%) and 20 µM (-78.6%) significantly ( $P \geq 0.001$ ) (Fig. 3A).

#### Expression of G9a gene

Figure 4 shows the expression of G9a gene and those associated with cell cycle proliferation after treatment of MCF-7 and HEK-293 with different concentrations of UNC0642.

The expression of G9a gene was downregulated in both cancerous and normal cell lines with increasing concentration of inhibitor UNC0642 (Fig. 4A). However, in case of HEK-293, at concentration 1 µM the expression of G9a gene upregulated as compared to their control (untreated). The cells treated with a higher concentration of inhibitor UNC0642 i.e., 20 µM showed 18-fold

downregulation as compared to control in the case of MCF-7 cell line and show 2.7-fold downregulation as compared to HEK-293 control. However, in the case of both cell lines, the changes in the G9a expression were significant ( $P < 0.05$ ) at higher concentrations of inhibitor.

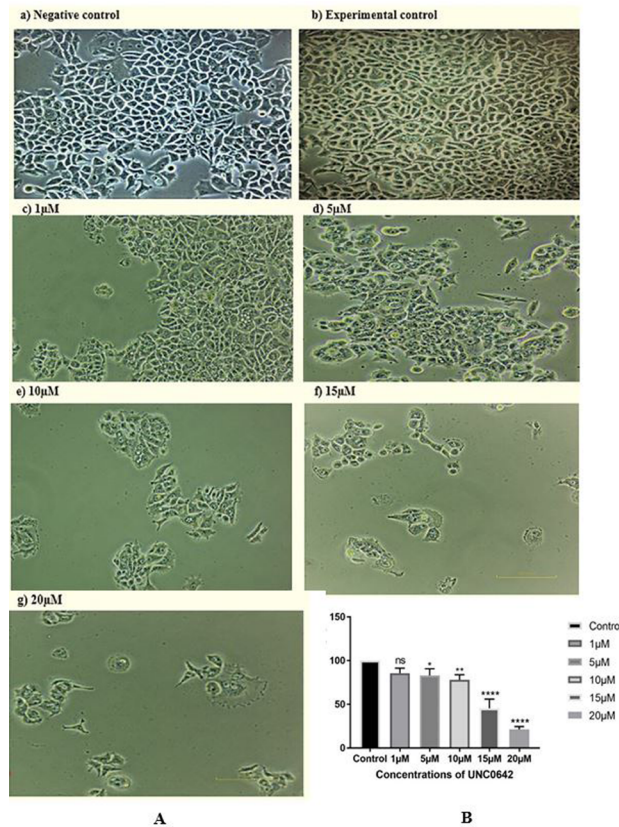


Fig. 3. Effect of different concentrations of inhibitor UNC0642 administered for 48 h on the morphology of MCF-7 cells (A) (a) Negative control (untreated cells); (b) Experimental control (treated with 0.05% DMSO supplemented medium); (c) 1 μM; (d) 5 μM; (e) 10 μM; (f) 15 μM; (g) 20 μM after 48 h treatment. The control cells showed normal morphology whereas UNC0642 treated cells exhibited stressed morphology with a significant decrease in the number of cells as the concentration of inhibitor is increased. (B) shows the effect of inhibitor on proliferation of MCF7 cells as determined by BrdU assay. The control cells were treated with 0.05% DMSO supplemented medium. See Figure 2 for statistical detail.

#### Expression of proliferation markers

Figure 4 also shows the effect of different concentration of UNC0642 on expression of proliferation markers such as CCND1, FGF1 and ENO2 in both the cell lines. The expression of cyclin D1 (CCND1) and FGF1 were significantly downregulated in both normal HEK-

293 and MCF-7 breast cancer cell lines after treatment with increasing concentrations of inhibitor. Although ENO2 follow almost the same trend as for the other two proliferation markers, but the ENO2 expression is more drastically downregulated in MCF-7 cells after treatment with the inhibitor at 10 μM, 15 μM and 20 μM concentration, whereas the non-cancerous normal HEK-293 cells do not seem to be affected much after inhibitor treatment.

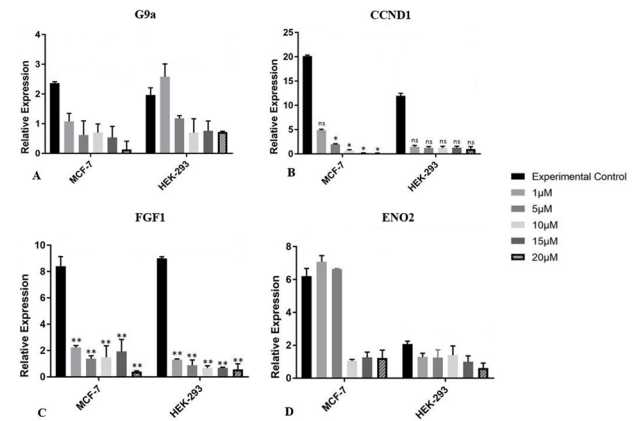


Fig. 4. Effect of different concentrations of inhibitor UNC0642 administered for 48 h on relative expression of G9a (A), Cyclin D1 (B), fibroblast growth factor 1 (C) and Enolase 2 (D) genes determined by real-time PCR using HMBS as a reference gene for normalization and negative control (untreated) as calibrator. Compared with the respective controls, treatment with higher concentrations of inhibitor downregulated the expression of G9a, CCND1, FGF1 and ENO2 genes in both the cell lines. For statistical details see Figure 2.

#### Expression of tumor suppressor genes

Figure 5 shows the effect of inhibitor on expression of tumor suppressor genes –AMPKα2 and ELL2 in MCF-7 and HEK-293 cells. Compared to the controls of MCF-7 and HEK-293, the expression of AMPKα2 gene was upregulated in both cancerous and normal cell lines with increasing concentration of inhibitor UNC0642 (Fig. 5A). However, in HEK-293 cells, treatment with higher concentrations of UNC0642 resulted in enhanced upregulation compared to the respective treatment in MCF-7 cells. Although the expression of the tumor suppressor gene was upregulated in the cancerous cells, but it was not to the extent as in non-cancerous cells.

The expression of ELL2 gene was upregulated after treatment with different concentrations of UNC0642 in both the cancerous and non-cancerous cells. The upregulation was however much more pronounced in MCF-7 cells than in HEK-293 cells (Fig. 5B). The increase in ELL2 expression in MCF-7 cells after treatment with

UNC0642 at concentration of 5, 10, 15 and 20  $\mu\text{M}$  was 10, 12, 14.5 and 15 fold respectively compared with the control, whereas in HEK-293 cells this increase was 4, 9, 10 and 11 fold respectively (Fig. 5B).

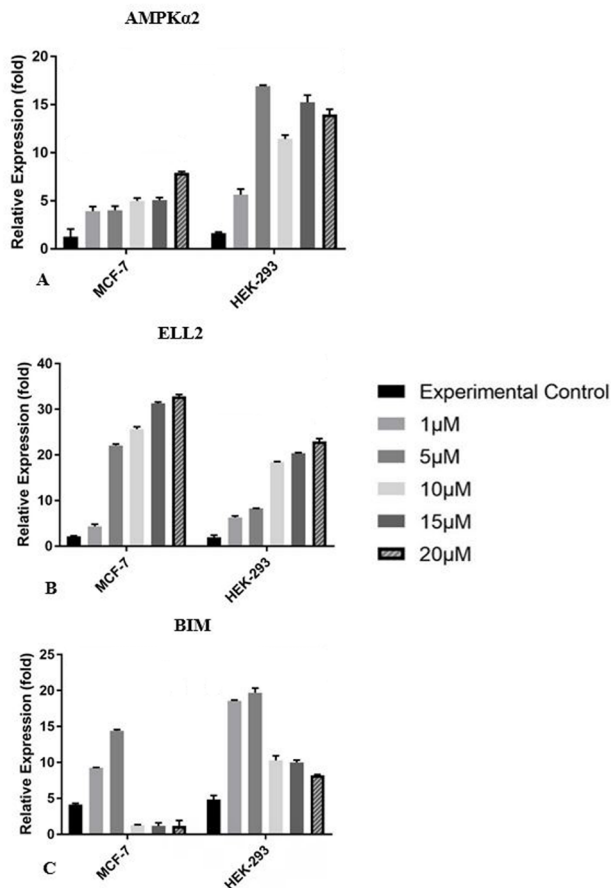


Fig. 5. Effect of different concentrations of inhibitor UNC0642 administered for 48 h on relative expression of AMPK $\alpha$ 2, ELL2 and Bcl-2 homology 3-only protein BIM genes determined by real-time PCR using HMBS as a reference gene for normalization and negative control (untreated) as calibrator. Compared with the respective controls, treatment with higher concentrations of UNC0642 upregulated the expression of AMPK $\alpha$ 2 and ELL2 genes. Lower concentrations of inhibitor upregulated BIM expression in both cancerous and non-cancerous cell lines, whereas the higher concentrations downregulated the BIM gene expression in both cell lines. Statistical analysis was performed by using Two-way ANOVA with Tukey's multiple comparison test.

#### Expression of proapoptotic proteins

Figure 5C shows the expression of Bcl-2 homology 3-only protein BIM in MCF-7 and HEK-293 cells. In MCF-7 cells, the level of expression of BIM gene was

upregulated in cells treated with lower concentrations (1  $\mu\text{M}$  and 5  $\mu\text{M}$ ) of inhibitor UNC0642, whereas it is downregulated at the concentration of 10  $\mu\text{M}$ , 15  $\mu\text{M}$ , and 20  $\mu\text{M}$  UNC0642 compared to the respective control. The expression of BIM in non-cancerous cells follow almost the same pattern after treatment with the inhibitor. The reduction in expression at higher concentrations of inhibitor is not as drastic as seen in the cancerous cells.

## DISCUSSION

G9a, a recently studied methylase is reported to play a vital role in many physiological processes including cancer progression. The expression levels of G9a are found to be highly upregulated in many types of cancers. As a result, G9a is considered a therapeutic target for cancer treatment. Studies have shown that G9a expression is increased in different types of multiple myeloma cell lines. In a group of patients with multiple myeloma, G9a expression predicts a poor prognosis. In multiple myeloma, G9a depletion decreased proliferation and tumorigenesis. Inhibition of G9a with UNC0642 resulted in a substantial reduction in RelB expression, which triggered transcription of the proapoptotic genes BIM and BMF and decreased proliferation and tumorigenesis. When RelB expression was restored, the reduction of proliferation and tumorigenesis induced by G9a deficiency was eliminated (Zhang *et al.*, 2020).

G9a plays an oncogenic role in ovarian cancer by epigenetically regulating the metastasis genes in hypoxic conditions (Kang *et al.*, 2018), promoting angiogenesis in cervical cancer by inducing angiogenic factors (Chen *et al.*, 2017). When G9a inhibitors are used to treat glioma cells, they become more receptive to temozolomide (TMZ). Cell proliferation in BTC (biliary tract cancer) and UBC (urinary bladder cancer) cells were inhibited by treating them with G9a inhibitors (Pangeni *et al.*, 2020). In ovarian cancer, overexpression of G9a silence the expression of tumor suppressors such as CDH1, DUSP5, SPRY4, and PPP1R15A. It also methylates the tumor suppressor p53, rendering it inactive. As a result, it is thought that targeting the activity of G9a by its inhibitors in cancer leads to the re-expression of cancer silencer genes (Wozniak *et al.*, 2007).

Because of its significant role, it has considered being a novel target for anti-cancer agents. For this purpose, various G9a inhibitors have been reported that have different pharmacokinetic properties including BIX01294, UNC0224, UNC0321, E72, UNC0638, and UNC0642. UNC0642 inhibited G9a with IC<sub>50</sub> of <2.5nM and has better selectivity and in vivo pharmacokinetics characteristics than other G9a-specific inhibitors, making

it a good candidate for animal studies (Liu *et al.*, 2011).

A study conducted on inhibitor UNC0642 in 2019, discovered that the cell viability was drastically reduced and cell death was triggered when the activity of G9a was targeted by the inhibitor UNC0642 in human bladder cancer cell lines T24 and J82 *in vitro*. T24, J82, and 5637 cells were dose-dependently (1–20  $\mu\text{M}$ ) reduced in viability by UNC0642 treatment, with  $\text{IC}_{50}$  values of  $9.85 \pm 0.41$ ,  $13.15 \pm 1.72$  and  $9.57 \pm 0.37$   $\mu\text{M}$ , respectively (Cao *et al.*, 2019).

To contextualize the therapeutic role of G9a in cancer treatment, breast cancer cell line MCF-7 was treated with UNC0642– a novel G9a inhibitor. All the working concentrations i.e., 1 $\mu\text{M}$ , 5 $\mu\text{M}$ , 10 $\mu\text{M}$ , 15 $\mu\text{M}$ , and 20 $\mu\text{M}$  of UNC0642 and experimental control was maintained in 0.05% DMSO, because at such lower concentration DMSO has a non-toxic effect on the cells. To check the effect of UNC0642 on the growth and proliferation parameters of cells different cell-based assays were performed. The results of neutral red assay suggested that the viability of cells was significantly ( $P \leq 0.05$ ) reduced as the concentration of inhibitor UNC0642 increased. Furthermore, the  $\text{IC}_{50}$  of UNC0642 was found to be 12.6 $\mu\text{M}$ . A similar dose-dependent trend in the cell proliferation in terms of DNA synthesis was assessed by BrdU assay, it was found that like the previous assay, UNC0642 significantly inhibited ( $P \leq 0.05$ ) the growth of cells at higher concentration because a decreasing cell proliferation was observed as the concentration of UNC0642 increased.

To further contextualize the effect of UNC0642 inhibitor on MCF-7 cells, we selected genes that are involved in proliferation i.e., fibroblast growth factor 1 (FGF1), enolase 2 (ENO2) cyclin D1 (CCND1), and apoptosis and tumor suppression i.e., catalytic subunit of AMP-activated protein kinase (Ampk $\alpha$ 2), RNA polymerase II transcription elongation factor ELL2 and a proapoptotic Bcl-2 homology 3-only protein BIM to study their expression levels in MCF-7 breast cancer cell line *in vitro*. Molecular-level analysis of *G9a*, *FGF1*, *ENO2*, *CCND1*, *AMPK $\alpha$ 2*, *BIM*, and *ELL2* genes was studied in inhibitor-treated MCF-7 breast cancer cell line by quantitative real-time PCR. In real time, we have used the negative control (untreated cells) as a calibrator and DMSO is used as a vehicle control and calibrated as 1 because it has no effect on the expression of cells. We did that so we can see what effect UNC0642 has on untreated control because we do not want to take control as 1 to compare a trend between untreated cells gene expressions vs inhibitor treated cells gene expressions. The human embryonic kidney cell line HEK-293 was used as a model for non-cancerous cells. Different concentrations of UNC0642 (ranging from 1 $\mu\text{M}$  to 20 $\mu\text{M}$ ) were given to both cell lines.

It was found that treatment of UNC0642 downregulated the expression of G9a gene which in normal cases is reported to be upregulated in breast cancer cell line MCF-7. Consistently, the mRNA expression of proliferative markers i.e., CCND1, ENO2, and FGF1 downregulated as the concentration of UNC0642 increased and the mRNA expression of genes involved in apoptosis and suppression of tumor i.e., ELL2 and AMPK $\alpha$ 2 upregulated as the concentration of UNC0642 increased compared to control cells. However, a proapoptotic protein BIM showed unusual behavior in the mRNA expression which was observed to be upregulated at lower concentrations i.e., 1 $\mu\text{M}$  and 5 $\mu\text{M}$ , and downregulated at higher concentrations i.e., 10 $\mu\text{M}$ , 15 $\mu\text{M}$ , and 20 $\mu\text{M}$  compared to control in MCF-7 cells. The downregulation in the expression of BIM gene may be due to the lower number of cells at higher concentrations of UNC0642 as observed in cell growth and proliferation assays.

Table II explained the fold change (increase or decrease) in the relative expression of genes in breast cancer cell line MCF-7. The arrow ( $\uparrow$ ) in the table shows the upregulation of the respective gene whereas, arrow ( $\downarrow$ ) indicated the downregulation in the expression of gene as compared to control.

**Table II. Effect of different concentrations of inhibitor UNC0642 on the changes in relative expression of G9a gene, cell proliferation marker genes (CCND1, FGF1, ENO2), tumor suppressor genes (AMPK $\alpha$ 2, ELL2) and apoptotic gene (BIM) in MCF-7 cell line. These changes have been determined in terms of fold change (increase or decrease) with reference to control (untreated cells).**

Genes	Concentrations of UNC0642				
	1 $\mu\text{M}$	5 $\mu\text{M}$	10 $\mu\text{M}$	15 $\mu\text{M}$	20 $\mu\text{M}$
<i>G9a</i>	2.2 $\downarrow$	3.8 $\downarrow$	3.4 $\downarrow$	4.4 $\downarrow$	18 $\downarrow$
<i>CCND1</i>	4 $\downarrow$	10 $\downarrow$	30 $\downarrow$	126 $\downarrow$	183 $\downarrow$
<i>FGF1</i>	4 $\downarrow$	6.1 $\downarrow$	5.6 $\downarrow$	4.3 $\downarrow$	21 $\downarrow$
<i>ENO2</i>	1.14 $\uparrow$	1.1 $\uparrow$	6 $\downarrow$	5 $\downarrow$	5 $\downarrow$
<i>AMPK<math>\alpha</math>2</i>	3.1 $\uparrow$	3.18 $\uparrow$	3.94 $\uparrow$	4.01 $\uparrow$	6 $\uparrow$
<i>ELL2</i>	2 $\uparrow$	10 $\uparrow$	12 $\uparrow$	14.5 $\uparrow$	15 $\uparrow$
<i>BIM</i>	2.2 $\uparrow$	3.5 $\uparrow$	3.2 $\downarrow$	3.56 $\downarrow$	3.53 $\downarrow$

Meanwhile, the mRNA expression level of all these genes in normal human embryonic kidney cells was also examined, the findings suggest that the expression of G9a gene and proliferative markers i.e., CCND1, ENO2, and FGF1 were downregulated as the concentration of UNC0642 increased whereas the expression of apoptosis and tumor suppressor genes, including BIM, ELL2,

AMPK $\alpha$ 2 upregulated by UNC0642 treatment. Table III explained the fold-change (increase or decrease) in the relative expression of genes in HEK-293 cell line.

**Table III. Effect of different concentrations of inhibitor UNC0642 on the changes in relative expression of *G9a* gene, cell proliferation marker genes (*CCND1*, *FGF1*, *ENO2*), tumor suppressor genes (*AMPK $\alpha$ 2*, *ELL2*) and apoptotic gene (*BIM*) in a non- cancerous kidney cell line HEK-293. These changes have been determined in terms of fold change (increase or decrease) with reference to control (untreated cells).**

Genes	Concentrations of UNC0642				
	1 $\mu$ M	5 $\mu$ M	10 $\mu$ M	15 $\mu$ M	20 $\mu$ M
<i>G9a</i>	1.3 $\uparrow$	1.7 $\downarrow$	2.8 $\downarrow$	2.6 $\downarrow$	2.7 $\downarrow$
<i>CCND1</i>	8 $\downarrow$	9.5 $\downarrow$	9.8 $\downarrow$	9 $\downarrow$	12 $\downarrow$
<i>FGF1</i>	7 $\downarrow$	10 $\downarrow$	13 $\downarrow$	13 $\downarrow$	16 $\downarrow$
<i>ENO2</i>	1.6 $\downarrow$	1.7 $\downarrow$	1.5 $\downarrow$	2 $\downarrow$	3 $\downarrow$
<i>AMPK<math>\alpha</math>2</i>	3 $\uparrow$	10 $\uparrow$	7 $\uparrow$	9 $\uparrow$	8.5 $\uparrow$
<i>ELL2</i>	3 $\uparrow$	4 $\uparrow$	9 $\uparrow$	10 $\uparrow$	11 $\uparrow$
<i>BIM</i>	3.8 $\uparrow$	4 $\uparrow$	2 $\uparrow$	2 $\uparrow$	1 $\uparrow$

## CONCLUSIONS

In conclusion, the lower concentrations of UNC0642 were found to be less cytotoxic for the cells with IC<sub>50</sub> of 12.6 $\mu$ M. Furthermore, molecular-level analysis of UNC0642 treatment with study of various proliferation and apoptotic marker genes revealed that UNC0642 treatment downregulated gene expression of cell proliferation marker genes in MCF-7 cells, whereas increased the expression of tumor suppressor genes in a dose-dependent fashion. Lower concentrations of UNC0642 caused overexpression of an apoptotic marker gene BIM, indicating that targeting G9a could be a feasible therapeutic strategy for breast cancer treatment. Further elucidation of the role of G9a gene in cancer progression with the study of associated signaling pathways, safety analyses are essential both *in vitro* and *in-vivo* to establish G9a inhibition as a therapeutic option for the treatment of cancer, specifically breast cancer.

### Data availability statement

All data generated or analyzed during this study are included in this published article.

### Funding

Research funds for this study were provided by the University of the Punjab. The researchers did not receive any specific grant from funding agencies in the public, commercial or not for profit sectors.

### Statement of conflict of interest

The authors have declared no conflict of interest.

## REFERENCES

- Ates, G., Vanhaecke, T., Rogiers, V., and Rodrigues, R.M., 2017. Assaying cellular viability using the neutral red uptake assay cell viability assays. *Springer, N. Y.*, **1601**: 19-26. [https://doi.org/10.1007/978-1-4939-6960-9\\_2](https://doi.org/10.1007/978-1-4939-6960-9_2)
- Cao, H., Li, L., Yang, D., Zeng, L., Yewei, X., Yu, B., Liao, G., and Chen, J., 2019. Recent progress in histone methyltransferase (G9a) inhibitors as anticancer agents. *Eur. J. med. Chem.*, **179**: 537-546. <https://doi.org/10.1016/j.ejmech.2019.06.072>
- Cao, YP., Sun, JY., Li, MQ., Dong, Y., Zhang, YH., Yan, J., Huang, RM., and Yan, X., 2019. Inhibition of G9a by a small molecule inhibitor, UNC0642, induces apoptosis of human bladder cancer cells. *Acta Pharmacol. Sin.*, **40**: 1076-1084. <https://doi.org/10.1038/s41401-018-0205-5>
- Casciello, F., Windloch, K., Gannon, F., and Lee, J.S., 2015. Functional role of G9a histone methyltransferase in cancer. *Front. Immunol.*, **6**: 487. <https://doi.org/10.3389/fimmu.2015.00487>
- Chen, R.-J., Shun, C.-T., Yen, M.-L., Chou, C.-H., and Lin, M.-C., 2017. Methyltransferase G9a promotes cervical cancer angiogenesis and decreases patient survival. *Oncotarget*, **8**: 62081-62098. <https://doi.org/10.18632/oncotarget.19060>
- Kang, J., Shin, S.-H., Yoon, H., Huh, J., Shin, H.-W., Chun, Y.-S., and Park, J.-W., 2018. FIH is an oxygen sensor in ovarian cancer for G9a/GLP-driven epigenetic regulation of metastasis related genes. *Cancer Res.*, **78**: 1184-1199. <https://doi.org/10.1158/0008-5472.CAN-17-2506>
- Kaniskan, H.U.M., Martini, M.L., and Jin, J., 2018. Inhibitors of protein methyltransferases and demethylases. *Chem. Rev.*, **118**: 989-1068. <https://doi.org/10.1021/acs.chemrev.6b00801>
- Kubicek, S., O'Sullivan, R. J., August, E. M., Hickey, E. R., Zhang, Q., Teodoro, M. L., Rea, S., Mechtler, K., Kowalski, J.A., Homon, C. A., Kelly, T.A. and Jenuwein, T., 2007. Reversal of H3K9me2 by a small-molecule inhibitor for the G9a histone methyltransferase. *Mol. Cell*, **25**: 473-481. <https://doi.org/10.1016/j.molcel.2007.01.017>
- Li, Q., Wang, L., Ji, D., Bao, X., Tan, G., Liang, X., Deng, P., Pi, H., Lu, Y., Chen, C., He, M., Zhang, L., Zhou, Z., Yu, Z., and Deng, A., 2021. BIX-01294, a G9a inhibitor, suppresses cell proliferation by inhibiting autophagic flux in nasopharyngeal

- carcinoma cells. *Investig. New Drugs*, **39**: 686-696. <https://doi.org/10.1007/s10637-020-01053-7>
- Liu, F., Barsyte-Lovejoy, D., Allali-Hassani, A., He, Y., Herold, J. M., Chen, X., Yates, C.M., Frye, S.V., Brown, P.J., Huang, J., Vedadi, M., Arrowesmith, C.H., and Jin, J., 2011. Optimization of cellular activity of G9a inhibitors 7-aminoalkoxy-quinazolines. *J. med. Chem.*, **54**: 6139-6150. <https://doi.org/10.1021/jm200903z>
- Pangeni, R.P., Yang, L., Zhang, K., Wang, J., Li, W., Guo, C., Yun, X., Sun, T., Wang, J., and Raz, D.J., 2020. G9a regulates tumorigenicity and stemness through genome-wide DNA methylation reprogramming in non-small cell lung cancer. *Clin. Epigen.*, **12**: 88. <https://doi.org/10.1186/s13148-020-00879-5>
- Rahman, Z., Bazaz, M.R., Devabattula, G., Khan, M.A., and Godugu, C., 2021. Targeting H3K9 methyltransferase G9a and its related molecule GLP as a potential therapeutic strategy for cancer. *J. Biochem. mol. Toxicol.*, **35**: 1-11. <https://doi.org/10.1002/jbt.22674>
- Savickiene, J., Treigyte, G., Stirblyte, I., Valiulienė, G., and Navakauskiene, R., 2014. Euchromatic histone methyltransferase 2 inhibitor, BIX-01294, sensitizes human promyelocytic leukemia HL-60 and NB4 cells to growth inhibition and differentiation. *Leuk. Res.*, **38**: 822-829. <https://doi.org/10.1016/j.leukres.2014.04.003>
- Simms, D., Cizdziel, P.E., and Chomczynski, P., 1993. TRIzol: A new reagent for optimal single-step isolation of RNA. *Focus*, **15**: 532-535.
- Stewart, B. W. and Kleihues, P., 2003. *World cancer report*. International Agency for Research on Cancer Press, Lyon, France, pp. 181-188.
- Tao, Z., Shi, A., Lu, C., Song, T., Zhang, Z., and Zhao, J., 2015. Breast cancer: epidemiology and etiology. *Cell Biochem. Biophys.*, **72**: 333-338. <https://doi.org/10.1007/s12013-014-0459-6>
- Wang, Q., Wang, X., Lai, D., Deng, J., Hou, Z., Liang, H., and Liu, D., 2018. BIX-01294 promotes the differentiation of adipose mesenchymal stem cells into adipocytes and neural cells in Arbas Cashmere goats. *Res. Vet. Sci.*, **119**: 9-18. <https://doi.org/10.1016/j.rvsc.2018.05.009>
- Wozniak, R., Klimecki, W., Lau, S., Feinstein, Y., and Futscher, B., 2007. 5-Aza-2'-deoxycytidine mediated reductions in G9A histone methyltransferase and histone H3 K9 dimethylation levels are linked to tumor suppressor gene reactivation. *Oncogene*, **26**: 77-90. <https://doi.org/10.1038/sj.onc.1209763>
- Zhang, X.Y., Rajagopalan, D., Chung, T.-H., Hooi, L., Toh, T.B., Tian, J.S., Rashid, M., Beta, M.S.N.R., Gu, M., Lim, J.J., Wang, W., Chng, W.J., Jha, S., and Chow, E.K.-H., 2020. Frequent upregulation of G9a promotes RelB-dependent proliferation and survival in multiple myeloma. *Exp. Hematol. Oncol.*, **9**: 1-17. <https://doi.org/10.1186/s40164-020-00164-4>
- Zhong, X., Chen, X., Guan, X., Zhang, H., Ma, Y., Zhang, S., Wang, E., Zhang, L., and Han, Y., 2015. Overexpression of G 9a and MCM 7 in oesophageal squamous cell carcinoma is associated with poor prognosis. *Histopathology*, **66**: 192-200. <https://doi.org/10.1111/his.12456>